 DOI: 10.1002/maco.201106102

Corrosion behaviour in physiological fluids of surface films formed on titanium alloys

J. C. Mirza Rosca, E. Vasilescu, P. Drob, C. Vasilescu* and S. I. Drob

The properties of the surface films formed on Ti and its Ti–5Al–4V and Ti–6Al–3.5Fe alloys by chemical (immersion in 10 M NaOH) and thermal treatment (500 °C) were studied in this paper. Their corrosion behaviour in Ringer solution was investigated. After treatments, the sample microhardness was measured. Also, the sample surfaces were observed by an optical microscope before and after immersion in Ringer solutions. The electrochemical behaviour of the surface films obtained by the chemical and thermal treatments was studied using the methods of the electrochemical impedance spectroscopy (EIS) and monitoring of open circuit potentials at different immersion periods (up to 60 days) in Ringer solution. Microhardness increased with the increasing loads for the studied materials, showing the existence of a compact protective layer. Microscopic observations exhibited more compact coatings after 60 days of exposure in Ringer solution, due to the formation of an apatite layer. EIS spectra revealed surface films with two layers: an inner, barrier protective layer and an outer, porous apatite layer. The impedance increases in time denoting that the films have grown by apatite nucleation. Also, EIS spectra showed that the complex treatment by chemical + heat method is the most efficiently. For the samples treated by the two processes (chemical + heat) the values of the open circuit potentials are nobler than of the chemical treated samples, denoting better protective, bioactive films.

1 Introduction

Commercially pure titanium and its alloys have been extensively used as biomedical implants because they have an excellent reputation for corrosion resistance and mechanical properties [1]. But, titanium and its alloys are usually bioinert and do not form a chemical bond with the bone. Therefore, for to improve their bioactivity, these materials have been coated with porous calcium phosphate and hydroxyapatite layers which have good ability to bond to the living bone [2–6].

A conventional method to increase the bioactivity is plasma spray of hydroxyapatite coatings [7, 8]. But, these coatings can delaminate during long-term implantation, can degrade and can lead to osteolysis [2].

E. Vasilescu, P. Drob, C. Vasilescu, S. I. Drob
Institute of Physical Chemistry "Ilie Murgulescu", Spl. Independentei 202, 060021 Bucharest (Romania)
E-mail: cora_vasilescu@yahoo.com

J. C. Mirza Rosca
Las Palmas de Gran Canaria University, 35017 Tafira (Spain)

Another method is to obtain porous, hydrated titanium oxide by chemical alkali treatment that after a subsequent heat treatment is able to form hydroxyapatite in body fluid [9–15]. Apatite formed at the interface between implant and bone can directly bond to the bone because it has a close composition with that of the bone; so, the implant becomes osteoinductive (bone bonding).

It results that titanium and its alloys could be converted into bioactive materials through specifically chemical and thermal treatments [16, 17]. Alkali treatment produces the formation of a sodium titanate hydrogel which induces the apatite nucleation in the biological liquids. Thermal treatment enhances the apatite forming ability and consolidates its bonding with the substrate.

The properties of the surface films formed on Ti and its Ti–5Al–4V and Ti–6Al–3.5Fe alloys by chemical (immersion in 10 M NaOH) and heat treatment (500 °C) were studied in this paper. Their corrosion behaviour after different immersion hours in Ringer solution was investigated.

2 Experimental

Titanium and its Ti–5Al–4V and Ti–6Al–3.5Fe alloys were obtained by vacuum melting. The samples for experiments were

realised from ingots by processing to disc form. The discs were polished to mirror finish with alumina paste of 0.1 μm. Then, the samples were treated by:

- chemical treatment by immersion in 10 M NaOH at 60 °C for 24 h (indicated by letter c);
- washed with distilled water and dried at 40 °C, during 24 h;
- thermal treatment by heating in oven at 500 °C for 24 h and then cooled in water (indicated by letter h);
- both chemical and heat treatment (indicated by letter ch).

After treatments the sample microhardness was measured by means of an indentation test (Remet HX-1000 microhardness tester). The microhardness measurements were performed tangentially to the sample surface along the diameter. Loads of 10, 25, 50 and 200 g at every 15 s were used. The average value for each sample expressed as hardness Vickers degree (HV) was obtained. Based on this average value, the corresponding depth was calculated with Equation (1):

$$d = \sqrt{\frac{1.854 \cdot P}{49 \cdot \mathrm{HV}}} \quad (1)$$

where d = depth in μm; P = load in g; HV = Vickers hardness.

The sample surfaces were observed by an optical microscope (Olympus PME 3). The samples were polished to mirror finish, ultrasonically cleaned with deionised water and etched in Kroll's reagent containing 10 ml of HF, 5 ml of HNO_3 and 85 ml of H_2O.

The electrochemical behaviour of the surface films obtained by the chemical and heat treatments was studied using the methods of the electrochemical impedance spectroscopy (EIS) [18–21] and monitoring of open circuit potentials at different immersion periods (up to 60 days) in Ringer solution [22–26].

For electrochemical impedance spectroscopy measurements, a conventional three-electrode electrochemical cell with a platinum grid as counter electrode and saturated calomel electrode (SCE) as reference electrode was used. AC impedance data were obtained at open circuit potential using a PAR 263A potentiostat connected with a PAR 5210 lock-in amplifier. The amplitude of the AC potential was 10 mV and single sine wave measurements at frequencies between 10^{-1} and 10^5 Hz were performed for each sample.

Open circuit potentials were monitored for 60 days (1440 h) using a Hewlett Packard multimeter.

All measurements were performed in Ringer solution of composition (g/l): NaCl – 6.8; KCl – 0.4; $CaCl_2$ – 0.2; $MgSO_4 \cdot 7H_2O$ – 0.2048; $NaH_2PO_4 \cdot H_2O$ – 0.1438; $NaHCO_3$ – 1; glucose – 1. The temperature of Ringer solution was kept at 37 ± 1 °C.

Table 1. Microhardness (HV) and depth (d) of the surface films formed on Ti

Load (g)	Ti		Ti_c		Ti_h		Ti_{ch}	
	HV	d (μm)	HV	d (μm)	HV	d (μm)	HV	d (μm)
10	172	1.48	189	1.41	203	2.16	250	1.23
25	197	2.19	218	2.68	222	2.92	233	2.01
50	200	3.68	215	2.96	237	2.82	271	2.64
200	203	6.10	236	5.66	242	5.59	285	5.15

Table 2. Microhardness (HV) and depth (d) of the surface films formed on Ti–5Al–4V alloy

Load (g)	Ti–5Al–4V		Ti–5Al–$4V_c$		Ti–5Al–$4V_h$		Ti–5Al–$4V_{ch}$	
	HV	d (μm)	HV	d (μm)	HV	d (μm)	HV	d (μm)
10	190	1.41	214	1.32	264	1.20	309	1.11
25	210	2.42	260	1.91	307	1.76	358	1.63
50	233	2.84	310	2.47	382	2.22	419	2.14
200	242	5.59	335	4.75	397	4.36	485	3.95

3 Results and discussion

3.1 Microhardness and average depth of the surface films

Microhardness increased with the increasing loads for the studied materials, showing the existence of a compact protective layer (Tables 1–3). For the same materials, the microhardness had the highest value for the films obtained by chemical (c) and chemical + heat treatment (ch), revealing that these two treatments produced the most compact films. The alloys had about the same values of the microhardness, proving that their films have the same structure, composition and properties. Comparing with titanium, the alloys presented higher values for their microhardness, i.e. better surface films.

3.2 The behaviour of surface films from microscopic observations

Because of the oxide films on the surfaces of Ti and its alloys are transparently, they have different colours due to the interference

Table 3. Microhardness (HV) and depth (d) of the surface films formed on Ti–6Al–3.5Fe alloy

Load (g)	Ti–6Al–3.5Fe		Ti–6Al–$3.5Fe_c$		Ti–6Al–$3.5Fe_h$		Ti–6Al–$3.5Fe_{ch}$	
	HV	d (μm)	HV	d (μm)	HV	d (μm)	HV	d (μm)
10	187	1.42	232	1.28	241	1.25	295	1.13
25	211	2.12	296	1.76	311	1.74	321	1.72
50	231	2.86	305	2.49	328	1.98	350	2.32
200	243	5.58	350	4.64	387	4.42	390	4.40

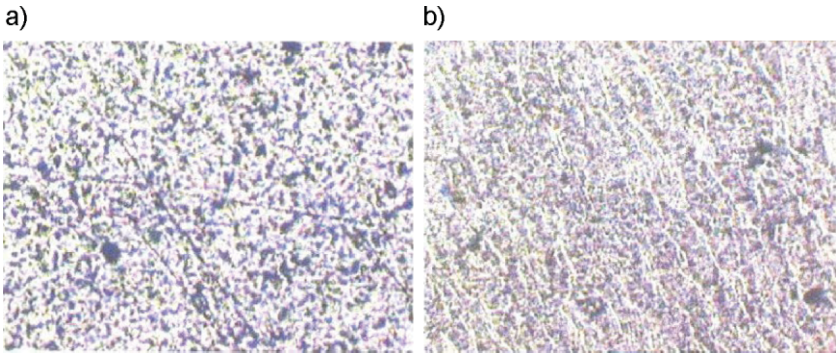

Figure 1. Aspects of Ti_{ch} samples before (a) and after 60 exposure days (b) in Ringer solution

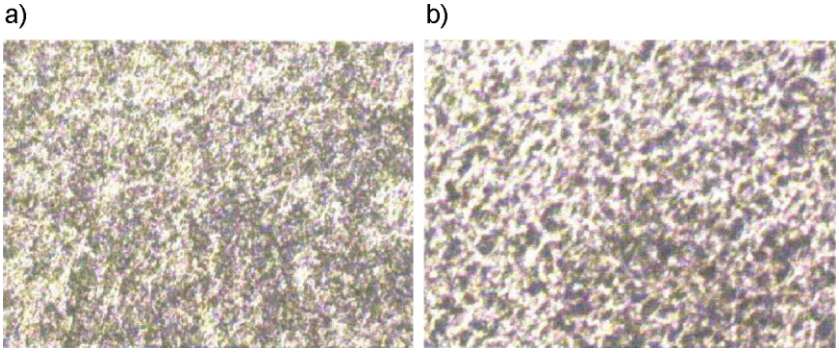

Figure 2. Aspects of $Ti–5Al–4V_{ch}$ alloy samples before (a) and after 60 exposure days (b) in Ringer solution

of the surface films with the incident light. Depending of their thickness and of light, these films are coloured in violet-blue, purple, bronze, brown, etc.

From Figures 1–3 it resulted the following:

- Ti_{ch}, chemical + heat treated presented a violet-blue coating before immersion (Fig. 1a) and a denser, violet-blue coating after 60 days of immersion in Ringer solution (Fig. 1b), attesting the formation of an apatite layer.
- $Ti–5Al–4V_{ch}$ alloy (Fig. 2) revealed a violet-green coating (Fig. 2a) before exposure and more compact violet-green coating (Fig. 2b) after 60 days of exposure in Ringer solution; this change of the aspect is due to the process of the apatite nucleation.
- $Ti–6Al–3.5Fe_{ch}$ alloy (Fig. 3) exhibited a violet-blue colour before immersion (Fig. 3a) and light violet-blue coating after 60 days of immersion in Ringer solution, as result of the apatite formation.

3.3 The behaviour of surface films from EIS spectra

The behaviour of the surface films was studied from Nyquist and Bode phase spectra obtained at different exposure periods in Ringer solution.

3.3.1 EIS spectra for titanium

Nyquist plots (Fig. 4) for titanium treated by chemical (c), heat (h) or chemical + heat (ch) methods show about incomplete semicircles with large diameters that increase with the exposure time; these semicircles denote a passive layer that improves its protective properties in time; also, these semicircles indicate a surface film with two layers. The highest impedance value was registered for the chemical + heat (ch) treated titanium, denoting the best protective properties.

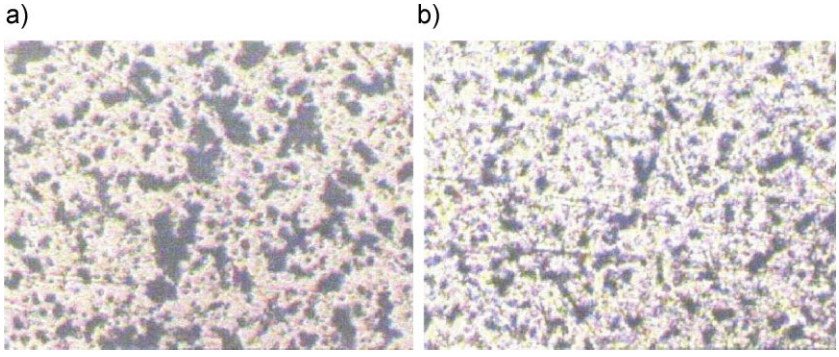

Figure 3. Aspects of $Ti–6Al–3.5Fe_{ch}$ alloy samples before (a) and after 60 exposure days (b) in Ringer solution

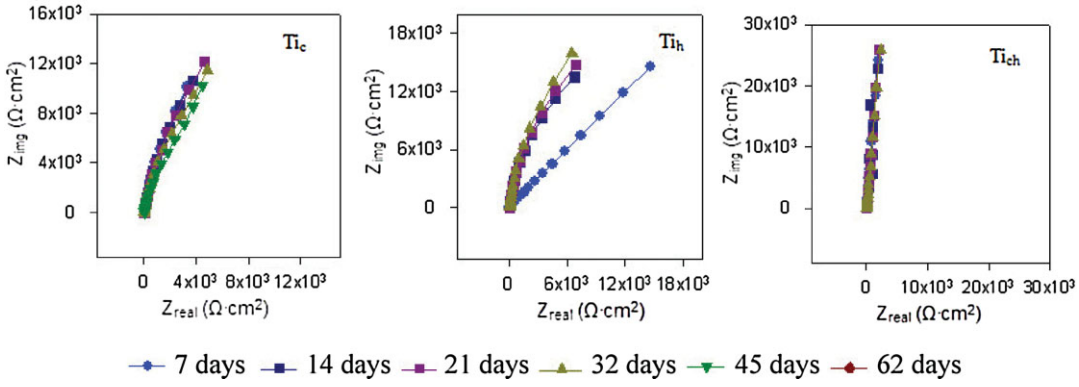

Figure 4. Nyquist plots for chemical, heat and chemical + heat treated Ti in Ringer solution

Bode phase plots (Fig. 5) exhibited two phase angles at almost −85°, typical for a capacitive, barrier layer represented by the passive titanium dioxide and another phase angle at about −40°, characterising a porous layer formed by the apatite deposited on the sample surfaces during their immersion in Ringer physiological solution [9, 13].

Kim et al. [27] and *Wang* et al. [13] proposed a mechanism of the apatite formation by alkali and heat treatments. In fact, during the alkali treatment, the porous TiO_2 layer dissolved forming negatively charged titanium hydrates and then an alkali titanate hydrogel. By heat treatment, this hydrogel layer is dehydrated and forms a stable amorphous or crystalline alkali titanate layer. By immersion in physiological fluid, the alkali titanate layer is again hydrated to transform into TiO_2 hydrogel by releasing alkali ions from the alkali titanate. This alkali release is essentially accompanying by ion exchange with H_3O^+ ion in human fluids, resulting in a pH increase in the surrounding fluid. This pH increase gives rise to an increase in the ionic activity product of apatite; so, appears the apatite nucleation; once the apatite nuclei are formed, they spontaneously grow, consuming the calcium and phosphorous ions from surrounding physiological fluid and so, the metallic implant becomes bioactively [28–31].

3.3.2 EIS spectra for Ti–5Al–4V alloy

For Ti–5Al–4V alloy, Nyquist plots (Fig. 6) show the same incomplete semicircles with large diameters increasing in time due to the improvement of the protective properties in the sequence: heat treated (h) < chemical treated (c) < chemical + heat treated (ch); taking into account the highest impedance values, it results that the best behaviour was obtained applying both treatments (chemical and heat).

Bode phase plots (Fig. 7) confirm the existence of surface films with two layers, by two phase angles: an angle at about −80°/−70° for inner, barrier passive layer and an angle at about −50°/−40° for outer, porous apatite layer. Phase angles changed in time due to the formation of the new apatite layer [9].

3.3.3 EIS spectra for Ti–6Al–3.5Fe alloy

For Ti–6Al–3.5Fe alloy, the same results were obtained: Nyquist plots (Fig. 8) revealed the same capacitive loops with the highest impedance values for chemical + heat treated (ch) alloy and the same increase of the impedance in time, denoting that the films have grown by apatite nucleation [9, 13]; Bode phase plots (Fig. 9) exhibited the same two phase angles, showing a film with two layers: an inner, barrier passive layer represented by a phase angle at about −80°/−85° and an outer porous apatite layer illustrated by a phase angle at −45°/−50°.

Similar results were obtained by *Raman* et al. [9] and *Krupa* et al. [15] for titanium during alkali, respectively, alkali and thermal treatments. They modelled an equivalent electric circuit with two time constants: the first time constant is for inner, barrier layer, responsible for the protective properties of the

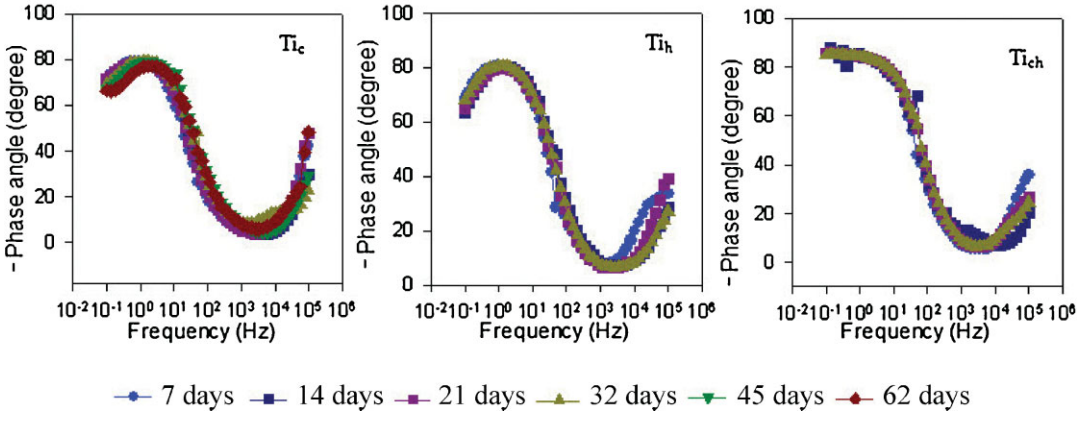

Figure 5. Bode plots for chemical, heat and chemical + heat treated Ti in Ringer solution

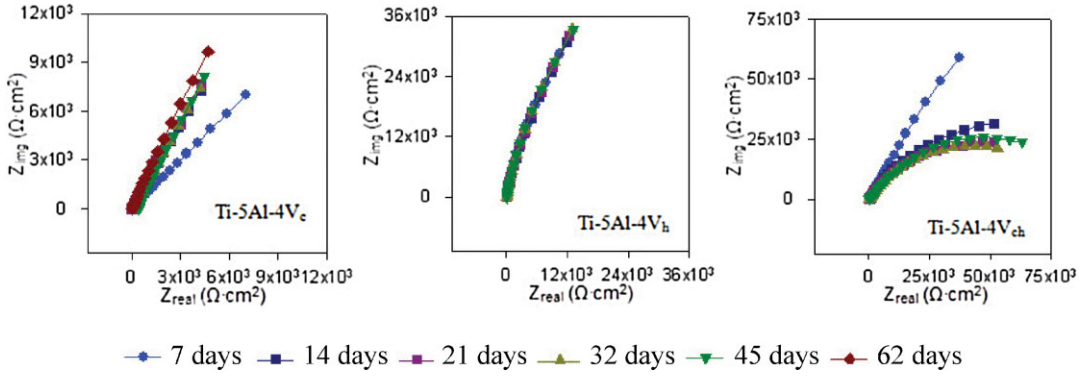

Figure 6. Nyquist plots for chemical, heat and chemical + heat treated Ti–5Al–4V alloy in Ringer solution

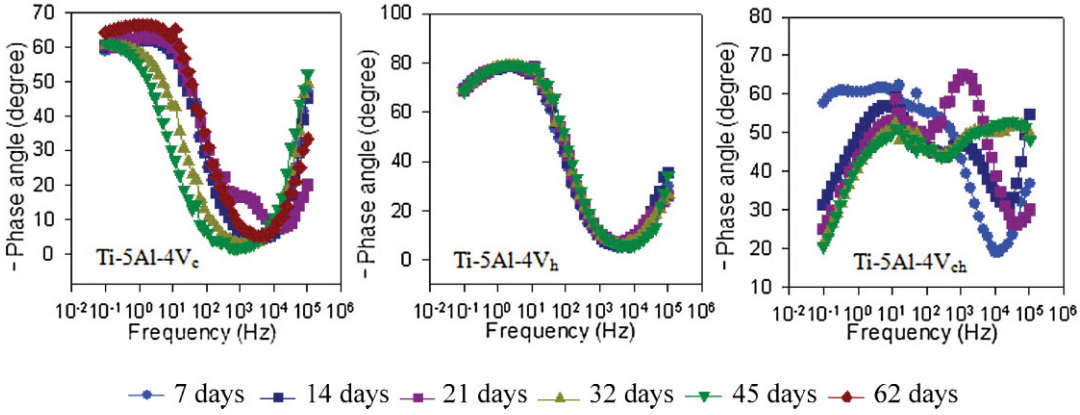

Figure 7. Bode plots for chemical, heat and chemical + heat treated Ti–5Al–4V alloy in Ringer solution

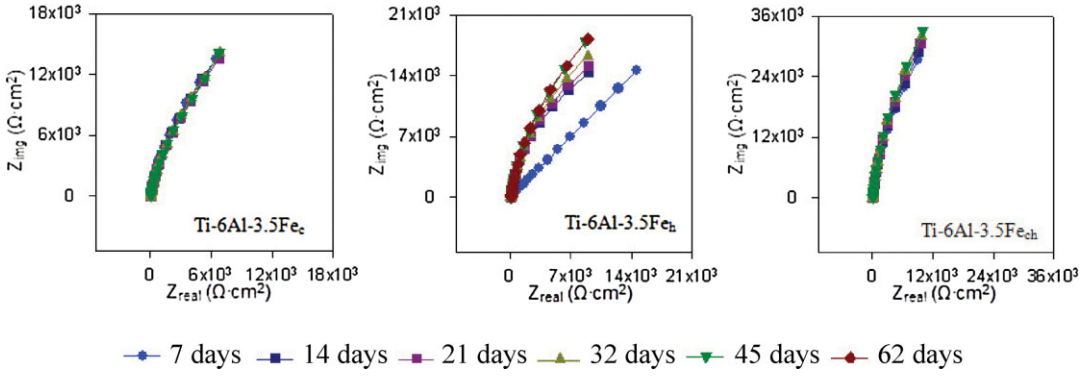

Figure 8. Nyquist plots for chemical, heat and chemical + heat treated Ti–6Al–3.5Fe alloy in Ringer solution

coating; the second time constant represents the outer, porous layer formed by apatite and is responsible for the bioactive properties of the coating.

3.4 The behaviour of the surface films from monitoring of the open circuit potentials

The open circuit potentials for treated Ti (Fig. 10), Ti–5Al–4V alloy (Fig. 11) and Ti–6Al–3.5Fe alloy (Fig. 12) presented electropositive values, placed on Pourbaix Diagrams [32] in the passive potential range. These open circuit potentials became nobler in time, showing that the surface films thickened in time [9, 33]. Because the values of the open circuit potentials continuously became more electropositive, it results that the processes of the thickening of the films take place during the whole immersion period of 60 days, i.e. the deposition of the apatite is permanently and un-interrupted. For the samples treated by the two processes (chemical + heat) the values of the open circuit potentials are nobler than of the chemical treated samples (Figs. 10–12), denoting better protective and bioactive films.

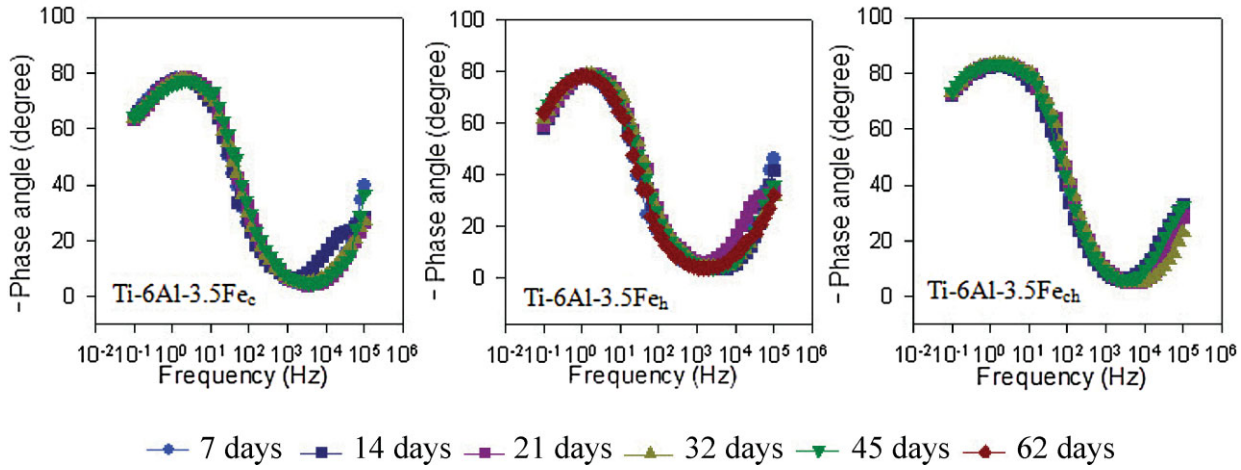

Figure 9. Bode plots for chemical, heat and chemical + heat treated Ti–6Al–3.5Fe alloy in Ringer solution

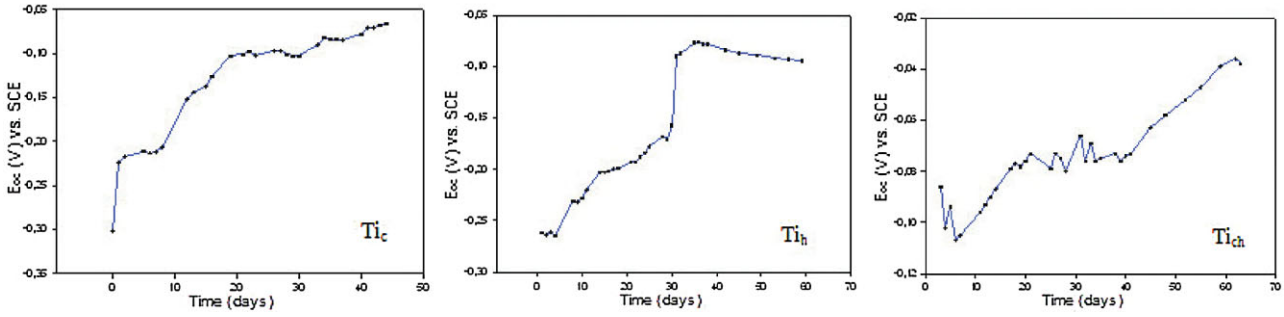

Figure 10. Open circuit potential *versus* time for chemical, heat and chemical + heat treated Ti in Ringer solution

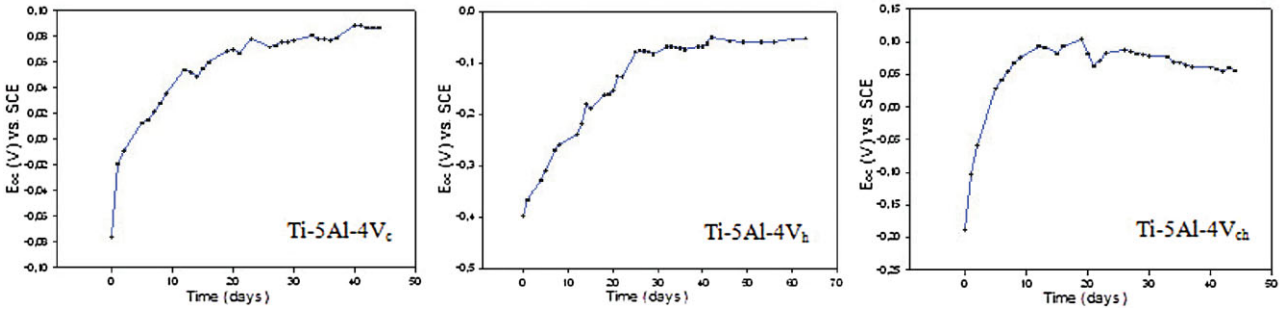

Figure 11. Open circuit potential *versus* time for chemical, heat and chemical + heat treated Ti–5Al–4V alloy in Ringer solution

4 Conclusions

The microhardness had the highest value for the films obtained by chemical (c) and chemical + heat (ch) treatments, revealing that these two treatments produced the most compact films. Comparing with titanium, the Ti–5Al–4V alloy and Ti–6Al–3.5Fe alloys presented higher values for their microhardness, i.e. better surface films.

Microscopic observations exhibited more compact coatings after 60 days of exposure in Ringer solution, due to the formation of the apatite layer.

EIS spectra obtained at different exposure periods in Ringer solution revealed surface films with two layers: an inner, barrier protective layer and an outer, porous apatite layer. The impedance increases in time denoting that the films have grown by apatite nucleation. The highest impedance values were obtained for chemical + heat treated (ch) alloys showing that this complex treatment is most efficiently.

The open circuit potentials presented electropositive values and became nobler in time, proving that the surface films thickened in time and the deposition of the apatite is permanently and un-interrupted. For the samples treated by the two processes

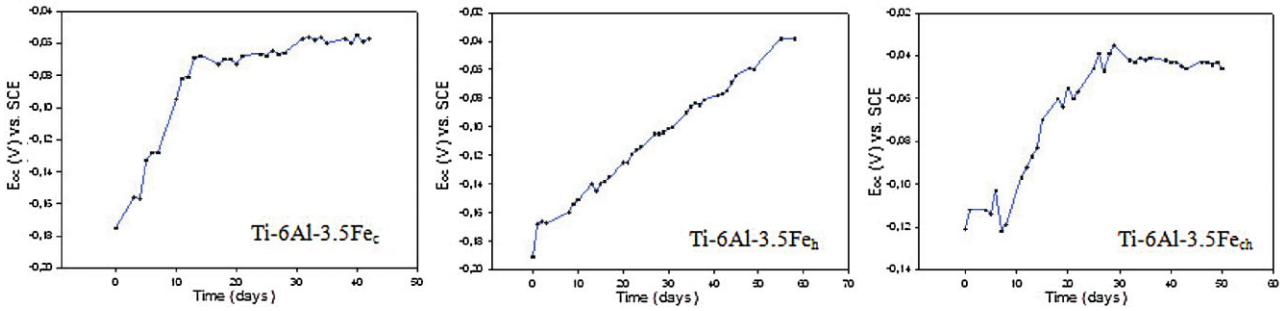

Figure 12. Open circuit potential *versus* time for chemical, heat and chemical + heat treated Ti–6Al–3.5Fe alloy in Ringer solution

(chemical + heat), the values of the open circuit potentials are nobler than of the chemical treated samples, denoting better protective and bioactive films.

Acknowledgements: This work was supported by Romanian CNCSIS – UEFISCDI, project number PN II – IDEI code 248/2010.

5 References

[1] A. Balamurugan, S. Rajeswari, G. Balossier, A. H. S. Rebelo, J. M. F. Ferreira, *Mater. Corros.* **2008**, *59*, 855.
[2] S. Fujibayashi, T. Nakamura, S. Nishiguchi, J. Tamura, M. Uchida, H. M. Kim, T. Kokubo, *J. Biomed. Mater. Res.* **2001**, *56*, 562.
[3] Q. Mohsen, S. A. Fadl-Allah, *Mater. Corros.* **2011**, *62*, 310.
[4] B. Feng, J. Y. Chen, S. K. Qi, L. He, J. Z. Zhao, X. D. Zhang, *J. Mater. Sci. Mater. Med.* **2002**, *13*, 457.
[5] S. Spriano, M. Bosetti, M. Bronzoni, E. Verne, G. Maina, V. Bergo, M. Cannas, *Biomaterials* **2005**, *26*, 1219.
[6] M. Javidi, M. E. Bahrololoom, S. Javadpour, J. Ma, *Mater. Corros.* **2009**, *60*, 336.
[7] Y. P. Lu, M. S. Li, S. T. Li, Z. G. Wang, R. F. Zhu, *Biomaterials* **2004**, *25*, 4393.
[8] R. B. Heimann, N. Schurmann, R. T. Muller, *J. Mater. Sci. Mater. Med.* **2004**, *15*, 1045.
[9] V. Raman, S. Tamilselvi, N. Rajendran, *Electrochim. Acta* **2007**, *52*, 7418.
[10] R. Godley, D. Starosvetsky, I. Gotman, *J. Mater. Sci. Mater. Med.* **2004**, *15*, 1073.
[11] X. Lu, Y. Lang, L. T. Wang, *J. Mater. Sci.* **2004**, *39*, 6809.
[12] V. Raghavan, *J. Phase Equilib.* **2002**, *23*, 182.
[13] C. X. Wang, M. Wang, X. Zhou, *Biomaterials* **2003**, *24*, 3069.
[14] A. K. Shukla, R. Balasubramanian, *Corros. Sci.* **2006**, *48*, 1696.
[15] D. Krupa, J. Baszkiewicz, J. W. Sobczak, A. Bilinski, A. Barcz, J. Mizera, *Proceedings of the 15th International Corrosion Congress*, Granada, Spain, **2002**, paper 523.
[16] X. X. Wang, S. Hayakawa, K. Tsuru, A. Osaka, *J. Biomed. Mater. Res.* **2000**, *52*, 171.
[17] M. Wei, H. M. Kim, T. Kokubo, J. H. Evans, *Mat. Sci. Eng. C-Biomim.* **2002**, *20*, 125.
[18] D. Mareci, R. Chelariu, D. M. Gordin, M. Romas, D. Sutiman, T. Gloriant, *Mater. Corros.* **2010**, *61*, 829.
[19] D. Mareci, R. Chelariu, G. Ciurescu, D. Sutiman, T. Gloriant, *Mater. Corros.* **2010**, *61*, 768.
[20] S. L. Assis, I. Costa, *Mater. Corros.* **2007**, *58*, 329.
[21] S. Tamilselvi, R. Murugaraj, N. Rajendran, *Mater. Corros.* **2007**, *58*, 113.
[22] M. V. Popa, I. Demetrescu, E. Vasilescu, P. Drob, A. Santana Lopez, J. Mirza-Rosca, C. Vasilescu, D. Ionita, *Electrochim. Acta* **2004**, *49*, 2113.
[23] E. Vasilescu, P. Drob, D. Raducanu, I. Cinca, D. Mareci, J. M. Calderon Moreno, M. Popa, C. Vasilescu, J. C. Mirza Rosca, *Corros. Sci.* **2009**, *51*, 2885.
[24] E. Vasilescu, P. Drob, C. Vasilescu, S. I. Drob, E. Bertrand, D. M. Gordin, T. Gloriant, *Mater. Corros.* **2010**, *61*, 947.
[25] E. Vasilescu, P. Drob, D. Raducanu, V. D. Cojocaru, I. Cinca, D. Iordachescu, R. Ion, M. Popa, C. Vasilescu, *J. Mater. Sci. Mater. Med.* **2010**, *21*, 1959.
[26] M. V. Popa, I. Demetrescu, S.-H. Suh, E. Vasilescu, P. Drob, D. Ionita, C. Vasilescu, *Bioelectrochemistry* **2007**, *71*, 126.
[27] H. M. Kim, F. Miyaji, T. Kokubo, T. Nakamura, *J. Biomed. Mater. Res.* **1996**, *32*, 409.
[28] C. X. Wang, M. Wang, K. Zhou, *Langmuir* **2002**, *18*, 7641.
[29] J. M. Shi, C. X. Ding, Y. H. Wu, *J. Inorg. Mat.* **2001**, *16*, 515.
[30] Q. L. Feng, F. Z. Cui, H. Wang, T. N. Kim, J. O. Kim, *J. Cryst. Growth* **2000**, *210*, 735.
[31] A. Bigi, M. Fini, B. Bracci, E. Boanini, P. Torricelli, G. Giavaresi, N. N. Aldini, A. Facchini, F. Sbaiz, R. Giardino, *Biomaterials* **2008**, *29*, 1730.
[32] M. Pourbaix, *Atlas of Electrochemical Equilibria in Aqueous Solutions*, NACE, Houston, **1974**.
[33] D. J. Blackwood, A. W. C. Chua, K. H. W. Seah, R. Thampuran, S. H. Teoh, *Corros. Sci.* **2003**, *42*, 481.

(Received: February 17, 2011) W6102
(Accepted: March 7, 2011)